The dynamics of a hole in a CuO₄ plaquette: electron energy-loss spectroscopy of Li₂CuO₂

S. Atzkern, M. Knupfer, M. S. Golden, and J. Fink Institut für Festkörper- und Werkstofforschung Dresden, P.O.Box 270016, D-01171 Dresden, Germany

C. Waidacher, J. Richter, and K. W. Becker Institut für Theoretische Physik, Technische Universität Dresden, D-01062 Dresden, Germany

N. Motoyama, H. Eisaki, and S. Uchida Department of Superconductivity, The University of Tokyo, Bunkyo-ku, Tokyo 113, Japan (November 22, 2018)

We have measured the energy and momentum dependent loss function of Li_2CuO_2 single crystals by means of electron energy-loss spectroscopy in transmission. Using the same values for the model parameters, the low-energy features of the spectrum as well as published Cu $2p_{3/2}$ x-ray photoemission data of Li_2CuO_2 are well described by a cluster model that consists of a single CuO₄ plaquette only. This demonstrates that charge excitations in Li_2CuO_2 are strongly localized.

PACS numbers: 71.27.+a, 71.45.Gm, 71.10.Fd

I. INTRODUCTION

At present a large variety of cuprate compounds with different element compositions and various crystal structures are known. The common structural unit of nearly all these materials is the square planar ${\rm CuO_4}$ plaquette with the oxygen atoms at the corners and the copper atom in the center. The ${\rm CuO_4}$ plaquettes can share oxygen atoms with their nearest neighbor plaquettes, thus building chains or planes. These ${\rm Cu-O}$ networks are separated generally by counter ions. Therefore, the electronic properties of the cuprates are low-dimensional.

For a given doping level, the arrangement of the plaquettes in the crystal is decisive in determining the mobility and correlation of the charge carriers. Therefore, it influences the particular physical properties of the cuprate compound under consideration. For instance, in many two-dimensional (2D) systems high- T_c superconductivity can be observed and among the quasi one-dimensional (1D) cuprates there exist excellent candidates for studying typically one-dimensional properties. Examples are the spin-Peierls transition which occurs in edge sharing chains $(CuGeO_3)^1$ or spin-charge separation in corner sharing chains $(Sr_2CuO_3)^{.2-4}$ Furthermore, in the spin ladder compounds the ordering of the CuO₄ plaquettes lies between 1D and 2D. Their magnetic properties change discontinuously with the transition from 1D to 2D.⁵ One example of such a system is Sr_{0.4}Ca_{13.6}Cu₂₄O₄₁ which consists of 2-leg ladders as well as chains of edge sharing plaquettes in alternating layers and which shows superconductivity under high pressure (3 GPa).⁶

In the hole picture (in the undoped case) every CuO_4 plaquette is occupied by a single hole in otherwise empty $Cu\ 3d$ and $O\ 2p$ orbitals. Thus, in the case of interconnected CuO_4 plaquettes the theoretical analysis of the

electronic structure has to deal with many-particle systems, and the interpretation of corresponding experimental data is rather complex. Furthermore, it is usually not possible to determine all theoretical model parameters for the Cu-O network from experiments. For these reasons it is helpful to study in detail the electronic properties of the structural unit, a single plaquette, itself to establish a basis for all Cu-O networks.

On the other hand, in real materials plaquettes are never truly isolated. Therefore, we have to choose a system in which the electronic interaction between the holes on the plaquettes and charge carriers in their vicinity can be estimated to be small. One candidate for such a system is Li_2CuO_2 . In view of the structure of Li_2CuO_2 (see Fig. 1), one might assign this compound to the 1D systems due to the parallel aligned chains of edge-sharing plaquettes. However, since the Cu-O-Cu-bond angle along the chains is almost 90°, the hopping from one plaquette to its nearest neighbor is strongly suppressed. Thus, although the magnetic interactions in Li_2CuO_2 are rather complex⁷⁻¹⁰, with respect to the electronic properties the plaquettes in this compound can be considered as approximately isolated.

Recently, the optical properties and the electronic structure of Li_2CuO_2 have been studied carrying out reflectivity¹¹, x-ray photoemission¹⁴ and x-ray absorption¹⁵ measurements. In this paper, we present transmission electron energy-loss spectroscopy (EELS) studies of Li_2CuO_2 . The resulting spectra allow us to study the multipole transitions between the ground state and the excited states of an approximately isolated single plaquette. Our theoretical analysis shows that the EELS results, as well as the Cu $2p_{3/2}$ x-ray photoemission spectrum published by Böske et al.¹⁴, can be described in a multi-band Hubbard model using the same

parameter values for the charge-transfer energy and the hopping amplitudes.

II. EXPERIMENTAL

Single crystals of Li_2CuO_2 were grown using a travelling solvent-zone technique. The crystal structure is shown in Fig. 1. Li_2CuO_2 has a body centered orthorhombic unit cell (space-group Immm) with the lattice constants a=3.661 Å, b=2.863 Å, and c=9.393 Å. Edge-sharing CuO_4 plaquettes lie in the (\mathbf{a},\mathbf{b}) plane and the chains are aligned along the \mathbf{b} direction. He Cu-O distance within the plaquette is 1.958 Å while the O-O distances in \mathbf{b} - and \mathbf{c} -direction are 2.863 Å and 2.671 Å, respectively. This configuration implies a Cu-O-Cu-bond angle of about 94°. The distances between a Cu in one chain and O atoms of neighboring chains are larger than 3 Å. This suggests that the electronic inter-chain coupling is small.

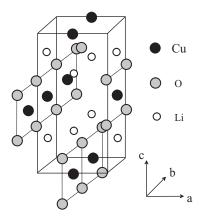


FIG. 1. Crystal structure of Li_2CuO_2 . The Cu atoms (black filled circles), and their nearest neighbor O atoms (grey filled circles) build chains of edge sharing CuO_4 plaquettes along **b**. The Li atoms (open circles) are located right below and above the Cu atoms in **c** direction.

Electron energy-loss spectroscopy (EELS) in transmission was performed on free standing films of about 1000 Å thickness which were cut from the crystals using an ultramicrotome with a diamond knife. All measurements were carried out at room temperature and with a momentum transfer parallel to the **b** and **c** axis. The primary beam energy was 170 keV. The energy resolution ΔE and the momentum transfer resolution Δq were chosen to be 110 meV and 0.05 Å⁻¹ for q \leq 0.4 Å⁻¹, and 160 meV and 0.06 Å⁻¹ for q \leq 0.4 Å⁻¹.

EELS provides us with the energy and momentum dependent loss function $\operatorname{Im}(-1/\varepsilon(\omega,\mathbf{q}))$ which is directly proportional to the imaginary part of the dynamical density-density correlation function

$$\chi_{\rho}(\omega, \mathbf{q}) = \frac{1}{i} \int_{0}^{\infty} dt \ e^{-i\omega t} \langle \Psi | [\rho_{-\mathbf{q}}(0), \rho_{\mathbf{q}}(t)] | \Psi \rangle \ . \tag{1}$$

 $|\Psi\rangle$ describes the ground state of the Hamiltonian, and $\rho_{\bf q}$ is the Fourier transformed hole density (see below). Equation (1) implies that for the limit ${\bf q} \to 0$ the selection rules for transitions are the same as in optics, i.e. dipole transitions are allowed. For finite ${\bf q}$ non-dipole transitions additionally contribute to the loss function.

III. RESULTS AND DISCUSSION

In Fig. 2 we show the loss function as well as the real part of the dielectric function, ε_1 , and the optical conductivity, $\sigma = \omega \varepsilon_0 \varepsilon_2$, of Li₂CuO₂ for a momentum transfer of $\mathbf{q} = 0.08 \text{ Å}^{-1}$. The latter two have been derived by a Kramers-Kronig analysis. The loss function is dominated by a broad feature around 21 eV which represents the volume plasmon, a collective excitation of all valence electrons. At lower energies several further plasmon excitations can be observed which are related to transitions between occupied and unoccupied electronic states with mainly Cu 3d, Cu 4s, and O 2p character. These transitions give rise to the maxima in the optical conductivity which is shown in the lower panel of Fig. 2. At small momentum transfers σ as derived from EELS can be directly compared to results from optical measurements. The optical conductivity of Li₂CuO₂ shown in Fig. 2 is in good agreement with recent optical studies. 11 Note that the corresponding maxima in the loss function are observed at higher energies when compared to the optical conductivity. This is a direct consequence of the collective nature of the plasmon excitations as observed in the loss function. 18

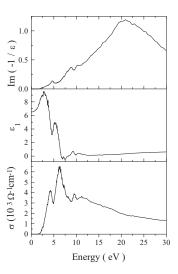


FIG. 2. Loss function, $\operatorname{Im}(-1/\varepsilon)$ (upper panel), real part of the dielectric function, ε_1 (middle panel), and optical conductivity, $\sigma = \omega \varepsilon_0 \varepsilon_2$ (lower panel) of Li₂CuO₂ for a small momentum transfer of 0.08 Å⁻¹ along the **b** direction.

Fig. 3a focusses on the loss function in a smaller energy range as a function of the momentum transfer. For small momentum transfer the energy range up to 6 eV is dominated by one distinct peak at 4.7 eV. With increasing **q** the intensity of this peak decreases while the intensity of a second feature around 5.7 eV, which becomes visible at $q \ge 0.7 \text{ Å}^{-1}$, increases. This behavior of the two features can be explained by the different multipole character of the corresponding transitions (see below). The steep rise of the background above 6 eV is due to the higher lying excitations (see Fig. 2).

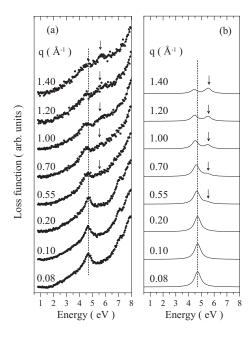


FIG. 3. Loss function of Li_2CuO_2 (left panel) measured with different momentum transfers \mathbf{q} parallel to the chain direction. The right panel shows the calculated dynamical density-density correlation function for the same \mathbf{q} values. The dashed lines and the arrows illustrate the small dispersion of the main peak and the increase of spectral weight with increasing \mathbf{q} around 5.5 eV, respectively.

Since the Cu-O-Cu-bond angle is close to 90°, the nearest-neighbor (NN) Cu-O-Cu hopping amplitude is small, and the delocalization properties of the system are dominated by a weak next-nearest neighbor (NNN) Cu-O-O-Cu hopping. In the loss function the NN as well as the NNN hopping might be visible in the tail of non-vanishing spectral weight between the spectral onset at $\sim 1.5~{\rm eV}$ and the main peak at 4.5 eV as has been discussed previously. However, in a first approximation the CuO4 plaquettes can be regarded as isolated and the charge excitations in the Cu-O network of Li₂CuO₂ as localized. This is supported by the small dispersion of the features in the EELS spectra which is in contrast to the strong positive dispersion of about 0.5 eV of the lowest lying excitations e.g. in the 1D system ${\rm Sr_2CuO_3}^4$ and in the 2D system ${\rm Sr_2CuO_2Cl_2.}^{12,13}$ In addition, the fact that the

spectra for \mathbf{q} parallel to the \mathbf{c} direction (not shown) are essentially identical to those for \mathbf{q} parallel to the \mathbf{b} direction also demonstrates the zero-dimensional character of the excitations.

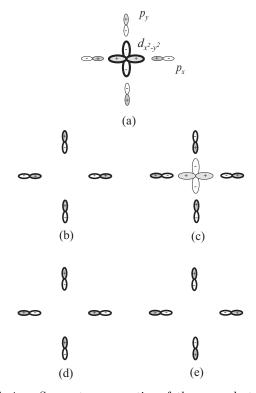


FIG. 4. Symmetry properties of the ground state (a), and the final states (b)-(e) of Hamiltonian(3). The relevant combinations of the hole occupied orbitals (Cu $3d_{x^2-y^2}$ and O $2p_{x,y}$) in the plaquette are shown. Thicker lines correspond to larger hole densities. The states (b), (d) and (e) have zero Cu weight. For momentum transfer parallel to the chain direction non-vanishing contributions come only from the final states (b) and (c).

Consequently, our model system for the calculation of the loss functions consists of a single CuO₄ plaquette only. This is a cluster with one Cu $3d_{x^2-y^2}$ orbital and four O $2p_{x(y)}$ orbitals (with site index $j=1,\ldots 4$), which is occupied by a single hole. The restriction to solely these orbitals is fully consistent with x-ray absorption measurements which indicate that the highest occupied states in Li₂CuO₂ have only small hole density in orbitals perpendicular to the CuO₄ plaquette. In this case, $\rho_{\bf q}$ has the form

$$\rho_{\mathbf{q}} = n^d + \sum_j n_j^p e^{i\mathbf{q}\mathbf{r}_j} , \qquad (2)$$

and the Hamiltonian reads

$$H = \Delta \sum_{j} n_{j}^{p} + t_{pd} \sum_{j} \phi_{j} \left(p_{j}^{\dagger} d + d^{\dagger} p_{j} \right)$$
$$+ t_{pp} \sum_{\langle j, j' \rangle} \phi_{jj'} p_{j'}^{\dagger} p_{j} . \tag{3}$$

 d^{\dagger} $\left(p_{i}^{\dagger}\right)$ creates a hole in the Cu 3d orbital (j-th O 2porbital), with occupation number operators n^d (n_i^p) . Δ is the charge-transfer energy. There are two hopping parameters: t_{pd} for the Cu-O hopping, and t_{pp} for the O-O hopping. The signs for the hopping are defined as follows: $\phi_1 = \phi_2 = -1$, $\phi_3 = \phi_4 = 1$, and $\phi_{jj'} = -\phi_j \phi_{j'}$. $\langle jj'\rangle$ denotes the summation over nearest neighbor pairs. Hamiltonian (3) is the simplest model which captures the essential features of the system. It can easily be solved exactly. The inclusion of anisotropic hopping will be discussed below.

Figure 4 shows the symmetry properties of the ground state (a), and the four excited states (b)-(e) of model (3). The ground state is a σ -bonding combination of the Cu $3d_{x^2-y^2}$ orbital and the four O 2p orbitals. Transitions into states (c) and (e) are optically forbidden. Thus, they only contribute to the loss function for finite momentum transfer. Moreover, if \mathbf{q} is parallel to the chain direction, non-vanishing contributions arise only from transitions into the final states (b) and (c). State (b) has pure O 2p character, whereas state (c) is the anti-bonding counterpart to (a). For $\mathbf{q} = 0$ dipole transitions into state (b) lead to spectral weight at energy ω_1 . A second excitation at energy ω_2 due to transitions into state (c) has non-vanishing weight for $\mathbf{q} \neq 0$:

$$\omega_1 = \frac{\Delta + 2t_{pp} + \omega_2}{2} , \qquad (4)$$

$$\omega_2 = \sqrt{(\Delta - 2t_{pp})^2 + 16t_{pd}^2} . \qquad (5)$$

$$\omega_2 = \sqrt{(\Delta - 2t_{pp})^2 + 16t_{pd}^2} \,. \tag{5}$$

These transitions, with energies ω_1 and ω_2 , appear as plasmon excitations in the EELS spectra at somewhat higher energies ω_1^{RPA} and ω_2^{RPA} . This effect is a result of the long-range Coulomb interaction (see also the discussion above). In the theoretical model this issue can be satisfactorily treated within the random-phase approximation (RPA).¹⁹

From the experimental spectrum we obtain for small momentum transfer $\omega_1^{\text{RPA}} = 4.7 \text{ eV}$ (see Fig. 3a). For larger q the experimental spectra show firstly a small negative dispersion of the main peak (see the deviation from the vertical dashed line in Fig. 3a) amounting to about 0.3 eV in the range between 0.1 and 1.4 Å^{-1} . This can be assigned to the decrease of the long-range Coulomb potential and the decreasing oscillator strength of the transition with increasing q. Secondly, the spectral weight between 5.5 and 5.8 eV (in Fig. 3a marked by arrows) is enhanced at higher q, resulting from the plasmon excitation related to the dipole forbidden transition at ω_2 . Since the excitation into the final state (c) corresponds to an octupole transition, the intensity of the corresponding feature in the EELS spectra is low at small q, and becomes visible only at rather high momentum transfers.

The two excitation energies ω_1 and ω_2 in equation (4) and (5) are described by the charge transfer energy Δ and the two hopping parameters t_{pd} and t_{pp} . Thus the energy positions of the two peaks observed in the EELS spectra do not yet determine the parameter set in a unique way. In order to remove the last degree of freedom in our model we use experimental evidence from Cu $2p_{3/2}$ core-level xray photoemission spectroscopy (XPS). Thereby we take advantage of the fact that three additional measured parameters in the XPS spectra, namely the energy positions as well as the ratio of the spectral weights of the main and satellite line are obtained, whereas only two variables are added to our model, namely the Coulomb repulsion U_{dc} and the exchange parameter I_{dc} . As explained in Ref. 20 for other compounds, we use model (3) to calculate the core level XPS of Li₂CuO₂. Good agreement with the experimental spectra¹⁴ is obtained if $t_{pd}^2/(\Delta-2t_{pp})$ lies between 0.7 and 0.8 eV.

It turns out that both the EELS and the XPS results can be described using one single parameter set for Hamiltonian (3): $\Delta = 2.7 \text{ eV}, t_{pd} = 1.25 \text{ eV}, \text{ and}$ $t_{pp} = 0.32 \text{ eV}^{21}$ which thus represents the most reliable parameter values for a CuO₄ plaquette in Li₂CuO₂. Our values for the charge-transfer energy Δ and the O-O hopping t_{pp} lie between those obtained from band-structure calculations⁷ ($\Delta = 2.5 \text{ eV}$, $t_{pp} = 0.25 \text{ eV}$), and from a fit to optical measurements¹¹ ($\Delta = 3.2 \text{ eV}$, $t_{pp} = 0.56 \text{ eV}$), while the value for t_{pd} is about 10% larger than in Refs. 7 and 11.

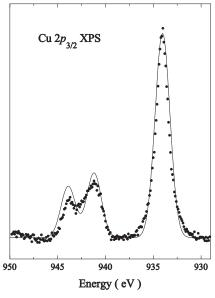


FIG. 5. Cu $2p_{3/2}$ photoemission spectrum of Li₂CuO₂, taken from Ref. 14. The solid line shows the theoretical results. Details of the calculation are described in Ref. 20.

In Figs. 3b and 5 the theoretical results are compared to the experimental EELS and XPS spectra. The theoretical spectra have been artificially broadened with a full width at half maximum of 0.6 eV for the EELS (Fig. 3b) and 1.8 eV for the XPS (Fig. 5). In agreement with the experimental result (Fig. 3a) the calculated EELS data for small momentum transfer consist of a single peak at $\omega_1^{\text{RPA}} = 4.7 \text{ eV}$. The energy $\omega_1 = 4.4 \text{ eV}$, calculated

with the parameter set received from our data, agrees well with the peak position in the optical conductivity as obtained performing a Kramers-Kronig analysis (see Fig. 2) and as derived from optical studies. 11 For increasing momentum transfer, the peak in the calculated loss function shows a small negative dispersion which is also in full agreement with the experiment. Furthermore, a second feature appears around $\omega_2^{\text{RPA}} = 5.5 \text{ eV}$, the symmetry properties of the associated final states have been discussed above. As regards the XPS results (Fig. 5), we also find a good agreement between theory and experiment. The structure of the experimental spectrum, which consists of a broad satellite (at higher binding energies) and a narrow main line, is correctly reproduced. In addition, the theoretical value for the ratio of the spectral weights of the satellite and the main line coincides with the experimental intensity ratio (0.56).¹⁴

We conclude with a short discussion of anisotropic hopping. In Li₂CuO₂, the O-O distance in chain direction (**b** direction) is about 7% larger than in **a** direction. Thus, one expects an anisotropy in the O-O hopping, with a larger hopping parameter t_{pp}^{\perp} perpendicular to the chain direction (see also Ref. 11). However, if **q** is parallel to the chain direction, a larger t_{pp}^{\perp} in the present model can be absorbed into a renormalized charge-transfer energy Δ without affecting the spectra. As the anisotropy of the edge-sharing CuO₄ plaquettes results in a finite Cu-O-Cu hopping to the next CuO₄ unit, an increase of this anisotropy causes a step towards a one-dimensional electronic system. This is actually realized in the related spin-Peierls compound CuGeO₃ where the anisotropy is about 16%. Thus, CuGeO₃ might be an ideal candidate for the investigation of the electronic structure of a system at the border to one dimension.

IV. SUMMARY

In summary, we have carried out EELS measurements of Li_2CuO_2 single crystals. Using the same model with the same parameter values, calculations of the energy and momentum dependent loss function of an isolated CuO_4 plaquette as well as of the $\text{Cu}\ 2p_{3/2}$ core-level XPS of Li_2CuO_2 agree well with the experimentally observed low-energy features of EELS as well as with published XPS data, respectively. Thus, a single parameter set for the charge-transfer energy ($\Delta=2.7~\text{eV}$), the copper-oxygen ($t_{pd}=1.25~\text{eV}$) and oxygen-oxygen ($t_{pp}=0.32~\text{eV}$) hopping amplitudes is sufficient to describe two independent experiments probing the electronic structure of Li_2CuO_2 in completely different energy ranges. These results confirm the strongly localized character of charge excitations in Li_2CuO_2 .

This work was supported by DFG through the research program of the SFB 463, Dresden.

- ¹ M. Hase, I. Terasaki and K. Uchinokura, Phys. Rev. Lett. **70**, 3651 (1993).
- ² E.H. Lieb and F.Y. Wu, Phys. Rev. Lett. **20**, 1445 (1968).
- ³ H. Fujisawa, T. Yokoya, T. Takahashi, S. Miyasaka, M. Kibune, and H. Takagi, Phys. Rev. B 59, 7358 (1999).
- ⁴ R. Neudert, M. Knupfer, M. S. Golden, J. Fink, W. Stephan, K. Penc, N. Motoyama, H. Eisaki, and S. Uchida, Phys. Rev. Lett. **81**, 657 (1998).
- ⁵ E. Dagotto and T.M. Rice, Science **271**, 618 (1996).
- ⁶ M. Uehara, T. Nagata, J. Akimitsu, H. Takahashi, N. Mori, and K. Kinoshita, J. Phys. Soc. Jpn. 65, 2764 (1996).
- ⁷ R. Weht and W.E. Pickett, Phys. Rev. Lett. **81**, 2502 (1998).
- ⁸ M. Boehm, S. Coad, B. Roessli, A. Zheludev, M. Zolliker, P. Böni, D. McK. Paul, H. Eisaki, N. Motoyama, and S. Uchida, Europhys. Lett. 43, 77 (1998).
- ⁹ V. Yu. Yushankhai and R. Hayn, Europhys. Lett. 47, 116 (1999).
- Y. Mizuno, T. Tohyama, and S. Maekawa, Phys. Rev. B 60, 6230 (1999).
- Y. Mizuno, T. Tohyama, S. Maekawa, T. Osafune, N. Motoyama, H. Eisaki, and S. Uchida, Phys. Rev. B 57, 5326 (1998).
- ¹² Y. Y. Wang, F. C. Zhang, V. P. Dravid, K. K. Ng, M. V. Klein, S. E. Schnatterly, and L. L. Miller, Phys. Rev. Lett. **77**, 1809 (1996).
- ¹³ R. Neudert, T. Böske, O. Knauff, M. Knupfer, M. S. Golden, G. Krabbes, J. Fink, H. Eisaki, and S. Uchida, Physica B 230-232, 847 (1997).
- ¹⁴ T. Böske, K. Maiti, O. Knauff, K. Ruck, M. S. Golden, G. Krabbes, J. Fink, T. Osafune, N. Motoyama, H. Eisaki, S. Uchida, Phys. Rev. B 57, 138 (1998).
- ¹⁵ R. Neudert, H. Rosner, S.-L. Drechsler, M. Kielwein, M. Sing, Z. Hu, M. Knupfer, M.S. Golden, J. Fink, N. Nücker, M. Merz, S. Schuppler, N. Motoyama, H. Eisaki, S. Uchida, M. Domke, G. Kaindl, Phys. Rev. B 60, 13413 (1999).
- ¹⁶ R. Hoppe and H. Riek, Z. Anorg. Allg. Chem. **379**, 157 (1970).
- ¹⁷ F. Sapiña, J. Rodriguez-Carvajal, M. J. Sanchis, R. Ibañez, A. Beltrán, and D. Beltrán, Solid State Commun. **74**, 779 (1990).
- ¹⁸ J. Fink, Adv. Electron Phys. **75**, 121 (1989).
- ¹⁹ See, e.g., D. Pines, *Elementary Excitations in Solids* (Addison-Wesley, Reading, MA, 1963), Chaps. 3-4.
- ²⁰ C. Waidacher, J. Richter, and K. W. Becker, Europhys. Lett. **47**, 77 (1999).
- The influence of the core hole in the XPS has been modelled using a Coulomb repulsion $U_{dc} = 8.35$ eV and an exchange parameter $I_{dc} = -1.5$ eV, consistent with other cuprates (see Ref. 20).